



**HAL**  
open science

## Structure–Function Analysis of the TssL Cytoplasmic Domain Reveals a New Interaction between the Type VI Secretion Baseplate and Membrane Complexes

Abdelrahim Zoued, Chloé J Cassaro, Eric Durand, Badreddine Douzi, Alexandre España, Christian Cambillau, Laure Journet, E. Cascales

### ► To cite this version:

Abdelrahim Zoued, Chloé J Cassaro, Eric Durand, Badreddine Douzi, Alexandre España, et al.. Structure–Function Analysis of the TssL Cytoplasmic Domain Reveals a New Interaction between the Type VI Secretion Baseplate and Membrane Complexes. *Journal of Molecular Biology*, 2016, 428 (22), pp.4413 - 4423. 10.1016/j.jmb.2016.08.030 . hal-01780163

**HAL Id: hal-01780163**

**<https://amu.hal.science/hal-01780163>**

Submitted on 27 Apr 2018

**HAL** is a multi-disciplinary open access archive for the deposit and dissemination of scientific research documents, whether they are published or not. The documents may come from teaching and research institutions in France or abroad, or from public or private research centers.

L'archive ouverte pluridisciplinaire **HAL**, est destinée au dépôt et à la diffusion de documents scientifiques de niveau recherche, publiés ou non, émanant des établissements d'enseignement et de recherche français ou étrangers, des laboratoires publics ou privés.

1     **Structure-function analysis of the TssL cytoplasmic domain reveals a new**  
2             **interaction between the Type VI secretion baseplate and membrane**  
3                     **complexes.**

4     Abdelrahim Zoued<sup>1,#</sup>, Chloé J. Cassaro<sup>1</sup>, Eric Durand<sup>1</sup>, Badreddine Douzi<sup>2,3,¶</sup>, Alexandre P.  
5     España<sup>1,†</sup>, Christian Cambillau<sup>2,3</sup>, Laure Journet<sup>1</sup>, and Eric Cascales<sup>1,\*</sup>

6  
7     <sup>1</sup> Laboratoire d'Ingénierie des Systèmes Macromoléculaires (LISM, UMR 7255), Institut de  
8     Microbiologie de la Méditerranée (IMM), Aix-Marseille Univ - Centre National de la Recherche  
9     Scientifique (CNRS), 31 chemin Joseph Aiguier, 13402 Marseille Cedex 20, France

10    <sup>2</sup> Architecture et Fonction des Macromolécules Biologiques (AFMB, UMR 6098), Centre National de  
11    la Recherche Scientifique (CNRS), Campus de Luminy, Case 932, 13288 Marseille Cedex 09, France.

12    <sup>3</sup> Architecture et Fonction des Macromolécules Biologiques (AFMB, UMR 6098), Aix-Marseille  
13    Univ, Campus de Luminy, Case 932, 13288 Marseille Cedex 09, France.

14    Present addresses:

15    <sup>#</sup> Howard Hughes Medical Institute, Brigham and Women's Hospital, Division of Infectious Diseases  
16    and Harvard Medical School, Department of Microbiology and Immunobiology, Boston,  
17    Massachusetts, USA

18    <sup>¶</sup> Laboratoire d'Ingénierie des Systèmes Macromoléculaires (LISM, UMR 7255), Institut de  
19    Microbiologie de la Méditerranée (IMM), Aix-Marseille Univ - Centre National de la Recherche  
20    Scientifique (CNRS), 31 chemin Joseph Aiguier, 13402 Marseille Cedex 20, France.

21    <sup>†</sup> Technological Advances for Genomics and Clinics laboratory (TAGC, U1090), Aix-Marseille Univ.  
22    - Institut National de la Santé et de la Recherche Médicale (INSERM), 163 Avenue de Luminy, 13288  
23    Marseille Cedex 09, France.

24  
25    \* corresponding author: [cascales@imm.cnrs.fr](mailto:cascales@imm.cnrs.fr)

26  
27    **Running head:** TssL structure-function analysis

28

## 1 Abstract

2 The Type VI secretion system (T6SS) is a multiprotein complex that delivers toxin effectors  
3 in both prokaryotic and eukaryotic cells. It is constituted of a long cytoplasmic structure - the  
4 tail - made of stacked Hcp hexamers and wrapped by a contractile sheath. Contraction of the  
5 sheath propels the inner tube capped by the VgrG spike protein towards the target cell. This  
6 tubular structure is built onto an assembly platform - the baseplate - that is composed of the  
7 TssEFGK-VgrG subunits. During the assembly process, the baseplate is recruited to a trans-  
8 envelope complex comprising the TssJ outer membrane lipoprotein and the TssL and TssM  
9 inner membrane proteins. This membrane complex serves as docking station for the  
10 baseplate/tail and as channel for the passage of the inner tube during sheath contraction. The  
11 baseplate is recruited to the membrane complex through multiple contacts including  
12 interactions of TssG and TssK with the cytoplasmic loop of TssM, and TssK interaction with  
13 the cytoplasmic domain of TssL, TssL<sub>Cyto</sub>. Here, we show that TssL<sub>Cyto</sub> interacts also with the  
14 TssE baseplate subunit. Based on the available TssL<sub>Cyto</sub> structures, we targeted conserved  
15 regions and specific features of TssL<sub>Cyto</sub> in enteroaggregative *Escherichia coli* (EAEC). By  
16 using bacterial two-hybrid and co-immunoprecipitation, we further show that the disordered  
17 L3-L4 loop is necessary to interact with TssK, that the L6-L7 loop mediates the interaction  
18 with TssE, whereas the TssM cytoplasmic loop binds the conserved groove of TssL<sub>Cyto</sub>.  
19 Finally, competition assays demonstrated that these interactions are physiologically important  
20 for EAEC T6SS function.

21

22 **Keywords:** Type VI secretion, protein-protein interaction, membrane complex, baseplate  
23 complex, loops, crevice, cleft.

24

# 1 Introduction

2 Bacteria have evolved strategies to survive within difficult environment or to  
3 efficiently colonize a specific niche. When nutrients become limiting or when conditions are  
4 defavorable, most Gram-negative Proteobacteria delivers anti-bacterial toxins into  
5 competitors. One of the main mechanisms for toxin delivery into prokaryotic cells is a  
6 multiprotein machinery called Type VI secretion system (T6SS).<sup>1-6</sup> The T6SS resembles a ~  
7 600-nm long cytoplasmic tail-like tubular structure anchored to the cell envelope, and works  
8 as a nano-crossbow.<sup>2,7,8</sup> The T6SS tail shares structural and functional homologies with  
9 contractile tail particles such as R-pyocins or bacteriophages.<sup>7-10</sup> The cytoplasmic tubular  
10 structure is constituted of an inner tube made of stacked Hcp hexamers organized head-to-tail  
11 and wrapped by a contractile sheath.<sup>7,9,11-17</sup> Contraction of the sheath propels the inner tube  
12 towards the target cell, allowing toxin delivery and target cell lysis.<sup>7,18-20</sup> This tubular  
13 structure is tipped by a spike, composed of a trimer of the VgrG protein and of the PAAR  
14 protein, which serves as puncturing device for penetration inside the target cell.<sup>9,21</sup> Toxin  
15 effectors are preloaded and different mechanisms of transport have been proposed, including  
16 cargo models in which effectors directly or indirectly binds on VgrG, PAAR or within the  
17 lumen of Hcp hexamers.<sup>3,6,21-29</sup>

18 The T6SS tail polymerizes on an assembly platform or baseplate complex (BC), which  
19 is also broadly conserved in contractile particles.<sup>30-34</sup> The composition of the T6SS baseplate  
20 has been recently revealed and is constituted of five proteins: TssE, TssF, TssG and TssK that  
21 assemble a complex together with the VgrG spike.<sup>32,33,35</sup> Once assembled in the cytoplasm,  
22 the BC is recruited and stabilized by a trans-envelope complex, or membrane complex (MC),  
23 constituted of TssJ, TssL and TssM subunits.<sup>32,36,37</sup> The structure and assembly of the MC are  
24 well known. TssJ is an outer membrane lipoprotein with a transthyretin fold<sup>38,39</sup>, whereas  
25 TssM and TssL are both anchored to the inner membrane. TssM is constituted of three trans-  
26 membrane helices (TMH) that delimitate a cytoplasmic loop between TMH2 and TMH3 and  
27 a large periplasmic domain downstream TMH3.<sup>40</sup> This periplasmic domain could be  
28 segmented into four sub-domains, the C-terminal one mediating contacts with TssJ.<sup>37,39</sup> By  
29 contrast, TssL has a single TMH located at its extreme C-terminus, and thus the majority of  
30 the protein protrudes into the cytoplasm.<sup>41</sup> The structures of the TssL cytoplasmic domains of  
31 enteroaggregative *E. coli* (EAEC), *Francisella tularensis* and *Vibrio cholerae* have been  
32 reported: they are composed of 7 helices grouped in two bundles, with an overall shape

1 resembling a hook.<sup>42-44</sup> The biogenesis of the MC starts with TssJ at the outer membrane and  
2 progresses with the sequential addition of TssM and TssL.<sup>37</sup> Ten copies of this heterotrimeric  
3 complex then combine to assemble a 1.7-MDa trans-envelope complex that serves both as  
4 docking station for the BC/tail structure and as channel for the passage of the inner tube  
5 during sheath contraction.<sup>32,37,45</sup> Recruitment of the BC to the MC is mediated by multiple  
6 interactions including interactions of TssG and TssK with the cytoplasmic domain of TssM,  
7 and of TssK with the cytoplasmic domain of TssL.<sup>32,46</sup>

8 Here, we conducted a structure-function analysis of the TssL cytoplasmic domain,  
9 TssL<sub>Cyto</sub>. We first demonstrate that, in addition to making contacts with the cytoplasmic  
10 domain of TssM and TssK, TssL<sub>Cyto</sub> interacts with the TssE baseplate component.  
11 Comparison of the EAEC, *F. tularensis* and *V. cholerae* TssL<sub>Cyto</sub> structures highlighted the  
12 presence of a cleft at the interface of the two-helix bundles with conserved negative charges.  
13 In addition, the two loops connecting helices 3-4 and 6-7 display significantly different shapes  
14 and/or flexibility. Site-directed mutagenesis coupled to protein-protein interaction studies  
15 demonstrated that the L3-4 and L6-7 loops mediate contact with the baseplate components  
16 TssK and TssE respectively, whereas the central cleft accommodates the TssM cytoplasmic  
17 domain. Finally, anti-bacterial assays showed that all these contacts are necessary for proper  
18 function of the Type VI secretion apparatus.

## 19 **Results**

### 20 **The TssL cytoplasmic domain, TssL<sub>Cyto</sub>, interacts with itself, the cytoplasmic loop of** 21 **TssM and the TssE and TssK baseplate components.**

22 Previous studies have demonstrated that the cytoplasmic domain of the  
23 enteroaggregative *Escherichia coli* TssL protein (EC042\_4527; Genbank accession (GI):  
24 **284924248**) forms dimers and interacts with the TssM and TssK proteins.<sup>40,42,46</sup> To gain  
25 further insights onto the interaction network of TssL<sub>Cyto</sub>, we performed a systematic bacterial  
26 two-hybrid (BACTH) analysis (Fig. 1A). As previously shown, we detected TssL<sub>Cyto</sub>  
27 interaction with itself, with TssK and with the cytoplasmic domain of TssM, TssM<sub>Cyto</sub>. In  
28 addition, this analysis revealed the interaction between TssL<sub>Cyto</sub> and the baseplate component  
29 TssE (Fig. 1A). The TssL<sub>Cyto</sub>-TssE interaction was further validated *in vitro* by using Surface  
30 Plasmon Resonance using purified proteins. TssE was covalently bound to the sensorchip and  
31 recordings were monitored after injection of increasing concentrations of TssL<sub>Cyto</sub> (Fig. 1B

1 and 1C). The sensorgrams confirmed the BACTH results and demonstrated that the two  
2 proteins interact with an affinity estimated to  $55 \pm 1.3 \mu\text{M}$  (Fig. 1B and 1C).

3

#### 4 **Structure analyses of TssL cytoplasmic domains.**

5 The crystal structures of the EAEC, *F. tularensis* and *V. cholerae* TssL cytoplasmic  
6 domains are available (PDB IDs: **3U66**<sup>42</sup>, **4ACL**<sup>43</sup> and **4V3I**<sup>44</sup>). All structures share common  
7 features (Fig. 2A; Supplementary Fig. S1): TssL<sub>Cyto</sub> is composed of 7  $\alpha$ -helices organized in  
8 two bundles constituted of helices  $\alpha$ 1-4 and  $\alpha$ 5-7. The  $\alpha$ 5-7 bundle is made of shorter helices  
9 in average, making an overall hook-like structure delimiting a cleft comprising conserved  
10 charged residues including aspartate 74 and glutamate 75 (Supplementary Fig. S1A).  
11 However, the three structures also highlighted significant differences, notably in loops L3-L4  
12 and L6-L7. TssL<sub>Cyto</sub> loop L3-L4 is disordered in *F. tularensis* whereas comprises a small  
13 additional  $\alpha$ -helix,  $\alpha$ A, in EAEC and *V. cholerae*. In addition, part of the L3-L4 loop  
14 structure could not be solved in the EAEC TssL<sub>Cyto</sub>, suggesting that this loop exhibits  
15 structural flexibility. TssL<sub>Cyto</sub> loop L6-L7 comprises an additional  $\alpha$ -helix,  $\alpha$ B, in *V. cholerae*,  
16 whereas adopts different conformations in EAEC and *F. tularensis* (Supplementary Fig. S1).  
17 These two loops having distinct structures, conformations or flexibility, they could be  
18 considered as interesting binding sites to confer specificity.

19

#### 20 **Mutagenesis of the charged cleft and L3-L4 and L6-L7 loops unveils contact zones with** 21 **TssM<sub>Cyto</sub>, TssK and TssE.**

22 To gain information on the role of the conserved cleft and of the L3-L4 and L6-L7  
23 loops, we engineered amino-acid substitutions in these different regions (Fig. 2B and Table  
24 1): (i) two charged residues (Glu-81 and Asp-84) within loop L3-L4 were converted to  
25 opposed charges (GluAsp-to-LysLys mutant, called hereafter EKDK) (orange arrows in Fig.  
26 2), (ii) small (Gly-137), aromatic (Phe-138) and charged (Asp-74 and Glu-75) chains within  
27 the cleft were substituted to yield Gly-to-Glu (GE), Phe-to-Glu (FE), GlyPhe-to-GluGlu  
28 (GEFE), Asp-to-Arg (DR), Glu-to-Arg (ER) and AspGlu-to-ArgArg (DRER) mutants (green  
29 arrows in Fig. 2), and (iii) three hydrophilic/charged residues within loop L6-L7 (Gln-145,

1 Asp-146 and Asp-147) were substituted with Lysine residues (GlnAspAsp-to-LysLysLys,  
2 QKDKDK) (blue arrows in Fig. 2).

3 These substitutions were first introduced into the TssL<sub>Cyto</sub>-T18 and pIBA-TssL<sub>Cyto</sub>  
4 vectors to test their impact on the interaction with TssE, TssK and the cytoplasmic loop of  
5 TssM, TssM<sub>Cyto</sub>, using bacterial two-hybrid and co-immunoprecipitation (Fig. 3). Two-hybrid  
6 analyses showed that none of these substitutions break the oligomerization of TssL<sub>Cyto</sub> (Fig.  
7 3A), in agreement with a previous study showing that TssL<sub>Cyto</sub> oligomerization is mediated by  
8 contacts between helices  $\alpha$ 1.<sup>42</sup> These results also suggest that each mutant variant is properly  
9 produced and does not present large structural changes compared to the wild-type TssL<sub>Cyto</sub>  
10 domain. The assay also revealed that most mutations within the TssL<sub>Cyto</sub> central cleft prevent  
11 formation of the TssL<sub>Cyto</sub>- TssM<sub>Cyto</sub> complex whereas substitutions within loops L3-L4 and  
12 L6-L7 abolish interaction with TssK and TssE, respectively (Fig. 3A).

13 These two-hybrid results were validated by co-immuno-precipitation analyses. Soluble  
14 lysates of cells producing the C-terminally FLAG-tagged wild-type TssL cytoplasmic domain  
15 and its substitution variants were combined with lysates containing VSV-G-tagged TssE,  
16 TssK and TssM<sub>Cyto</sub>. TssL<sub>Cyto</sub>-containing complexes were immobilized on agarose beads  
17 coupled to the monoclonal anti-FLAG antibody. Figure 3B shows that the wild-type TssL<sub>Cyto</sub>  
18 domain co-precipitates TssE, TssK and TssM<sub>Cyto</sub>. Each TssL<sub>Cyto</sub> variant is produced and  
19 immuno-precipitated at levels comparable to the wild-type TssL<sub>Cyto</sub> domain. Mutation of the  
20 Glu-Asp (EKDK mutant) and Gln-Asp-Asp (QKDKDK mutant) motifs within the L3-L4 and  
21 L6-L7 loops prevented interaction with TssK and TssE respectively, whereas most  
22 substitutions within the conserved groove abolished interaction with the TssM cytoplasmic  
23 domain (Fig. 3B).

24

25 **TssL<sub>Cyto</sub> interactions with TssE, TssK and TssM<sub>Cyto</sub> are critical for proper function of**  
26 **the Type VI secretion apparatus.**

27 The EAEC Sci-1 T6SS is involved in inter-bacterial competition by delivering Tle1, a  
28 toxin with phospholipase activity into competitor cells.<sup>27</sup> We therefore tested whether  
29 substitutions that abolish TssL<sub>Cyto</sub> complexes formation impact the function of the T6SS. The  
30 substitutions were introduced into the pOK-TssL vector, that encodes the full length TssL  
31 protein and previously shown to fully complement the  $\Delta$ tssL phenotypes.<sup>41</sup> The anti-bacterial

1 activity was tested against a competitor strain engineered to constitutively express the GFP  
2 and to resist kanamycin. The fluorescence levels of mixture containing the EAEC and  
3 competitor strains at a 4:1 ratio, which is proportional to the number of competitor cells was  
4 measured after 4 hours of contact. In addition, the survival of the competitor strain was  
5 measured by counting fluorescent colony-forming units (cfu) after plating serial dilutions of  
6 the mixture on plates supplemented with kanamycin. The results represented in Figure 4 show  
7 that the growth of the competitor strain was inhibited by the  $\Delta tssL$  strain producing the wild-  
8 type TssL protein, at a level comparable to that of the wild-type strain. By contrast, the  $\Delta tssL$   
9 strain did not cause growth inhibition of competitor cells. With the exception of the FE  
10 mutant strain, all the TssL variants were unable to complement the anti-bacterial defects of  
11 the  $\Delta tssL$  strain, demonstrating the formation of TssL<sub>Cyto</sub>-TssE, TssL<sub>Cyto</sub>-TssK and TssL<sub>Cyto</sub>-  
12 TssM<sub>Cyto</sub> complexes is necessary for proper assembly and function of the EAEC Sci-1 T6SS.

13

## 14 Discussion

15 In this study, we have used a systematic bacterial two-hybrid approach to define the  
16 partners of the T6SS TssL cytoplasmic domain. In addition to the known interacting subunits,  
17 TssM<sup>40</sup> and TssK<sup>46</sup>, we have found an additional contact with the TssE protein, a component  
18 of the baseplate. This interaction was confirmed *in vitro* using surface plasmon resonance.  
19 With the identification of TssM<sub>Cyto</sub>-TssG, TssM<sub>Cyto</sub>-TssK and TssL<sub>Cyto</sub>-TssK contacts<sup>32,46,47</sup>,  
20 the interaction of TssL<sub>Cyto</sub> with TssE corresponds to the fourth interaction between the T6SS  
21 membrane and baseplate complex. The cytoplasmic domain of TssL is located at the base of  
22 the TssJLM complex<sup>37</sup>, a location compatible with the position of the baseplate *in vivo*.<sup>7,32,48</sup>  
23 Although these interactions are of low affinity between isolated molecules (the dissociation  
24 constant measured *in vitro* for the TssL<sub>Cyto</sub>-TssE interaction is ~ 50 μM), the avidity should  
25 increase within the secretion apparatus by the number of interactions and the local  
26 concentration. Furthermore, the existence of four contacts likely stabilizes the recruitment of  
27 the baseplate to the membrane complex. These multiple contacts are probably important to  
28 properly position the baseplate onto the membrane complex and to maintain the baseplate  
29 stably anchored when the sheath contracts. In addition, it has been shown that the  
30 bacteriophage T4 baseplate is subjected to large conformational changes during sheath  
31 contraction<sup>33,49</sup>, and a similar situation is likely to occur in the case of the T6SS.<sup>30,32</sup> Therefore

1 it might be critical to have a multitude of contacts between the baseplate and membrane  
2 complexes as several interactions might be broken during the conformational transition.

3 TssL dimerizes and interacts with three proteins of the secretion apparatus (Fig. 5). In  
4 enteroaggregative *E. coli*, TssL dimerization occurs mainly by the trans-membrane segment  
5 with contribution of residues from helix  $\alpha$ 1. In this study, we provided further molecular  
6 details on the TssL interaction by conducting a structure-function analysis. First, using  
7 sequence alignment, we defined that a number of residues share high level of conservation.  
8 Interestingly, most of these residues locate at the interface between the two-helix bundles and  
9 delimitate a cleft. Second, by comparing the three available crystal structures of TssL  
10 cytoplasmic domains (from EAEC, *F. tularensis* and *V. cholerae*), we targeted two loops,  
11 loops L3-L4 and L6-L7, which present different shapes, distinct secondary structures  
12 (addition of short helices) and are highly degenerated. Substitutions were introduced in the  
13 cleft as well as in loops L3-L4 and L6-L7 and were tested for their impact on the interactions.  
14 None of these mutations disrupted the oligomerization of TssL<sub>Cyto</sub> suggesting that their impact  
15 on TssL<sub>Cyto</sub> folding was null or moderated. Our data show that the cleft is required for proper  
16 interaction with TssM<sub>Cyto</sub>, whereas loops L3-L4 and L6-L7 are putative binding sites for TssK  
17 and TssE respectively. The conservation of the charged crevice in TssL proteins suggests that  
18 the mode of binding of TssL/TssM proteins might be conserved. It is worthy to note that the  
19 T6SS-associated TssL and TssM proteins share homologies with IcmH/DotU and IcmF, two  
20 subunits of the *Legionella pneumophila* Type IVb secretion system (T4bSS).<sup>8,42</sup> Interestingly,  
21 IcmH/DotU also possesses charged residues in the putative cleft position, suggesting that this  
22 cleft might also be important for binding to IcmF. By contrast, the variability of the L3-L4  
23 and L6-L7 loops might confer specificity between TssL proteins and the baseplate complex,  
24 notably when different T6SS are produced simultaneously in a bacterium. However, while our  
25 results demonstrate that these regions are necessary for these interactions, it remains to be  
26 defined whether these regions are sufficient. Swapping experiments between TssL proteins  
27 from different bacteria would be an interesting extension of this study. Finally, these data are  
28 interesting for the development of inhibitors that will target the assembly of the membrane  
29 complex or the recruitment of the baseplate. Specifically, crevices such as the cleft that  
30 accommodates the TssM cytoplasmic domain are interesting targets for drugs, while mimetic  
31 peptides might be used to prevent interaction of the baseplate components with the TssL  
32 loops.

1

## 2 MATERIALS and METHODS

3 **Bacterial strains and media.** The *Escherichia coli* K-12 DH5 $\alpha$ , BTH101, W3110 and BL21(DE3)  
4 pLysS strains were used for cloning procedures, bacterial two-hybrid analyses, co-  
5 immunoprecipitations and protein production, respectively. Strain W3110 pUA66-*rrnB* (Kan<sup>R</sup>,  
6 constitutively expressing the Green Fluorescent Protein [GFP])<sup>50,51</sup> was used as prey in anti-bacterial  
7 competition experiments. Enteroaggregative *E. coli* (EAEC) strain 17-2 has been used as source of  
8 DNA for PCR amplification, and for phenotypic analyses. The  $\Delta$ *tssL* 17-2 derivative mutant strain has  
9 been previously described.<sup>36</sup> Cells were grown in Lysogeny broth (LB), Terrific Broth (TB) or Sci-1-  
10 inducing medium (SIM)<sup>52</sup> as specified. Plasmids were maintained by the addition of ampicillin (100  
11  $\mu$ g/mL), chloramphenicol (40  $\mu$ g/mL) or kanamycin (50  $\mu$ g/mL for *E. coli* K-12 and 100  $\mu$ g/mL for  
12 EAEC). Expression of genes cloned into pOK12, pASK-IBA37+, pBAD33 and pETG20A vectors  
13 were induced by the addition of isopropyl-thio- $\beta$ -D-galactopyranoside (IPTG; 50  $\mu$ M in liquid, 10  
14  $\mu$ M on agar plates), anhydrotetracyclin (AHT; 0.1  $\mu$ g/mL), L-arabinose (0.2%) and IPTG (0.5 mM),  
15 respectively.

16 **Plasmid construction.** Plasmids used in this study are listed in Supplemental Table S1. Polymerase  
17 Chain Reactions (PCR) were performed using a Biometra thermocycler using the Q5 high fidelity  
18 DNA polymerase (New England BioLabs). Custom oligonucleotides, listed in Supplemental Table S1,  
19 were synthesized by Sigma Aldrich. Enteroaggregative *E. coli* 17-2 chromosomal DNA was used as a  
20 template for all PCRs. The amplified DNA fragments correspond to the full-length or the cytoplasmic  
21 domain (TssL<sub>Cyto</sub>, residues 1-184)<sup>41</sup> of TssL (EC042\_4527, GI: 284924248), the full-length TssK  
22 (EC042\_4526, GI: 284924247) and TssE (EC042\_4545, GI: 284924266) proteins, and the  
23 cytoplasmic domain (TssM<sub>Cyto</sub>, residues 62-360) of the TssM protein (EC042\_4539, GI: 284924260).  
24 The pOK-TssL plasmid, producing the full-length TssL proteins fused to a C-terminal HA epitope and  
25 plasmids pETG20A-TssL<sub>Cyto</sub> and pETG20A-TssE have been previously described.<sup>41,42,45</sup> pASK-  
26 IBA37+, pBAD33 plasmid derivatives were engineered by restriction-free cloning<sup>53</sup> as previously  
27 described.<sup>36</sup> Briefly, genes of interest were amplified with oligonucleotides introducing extensions  
28 annealing to the target vector. The double-stranded product of the first PCR was then been used as  
29 oligonucleotides for a second PCR using the target vector as template. Codon substitutions have been  
30 obtained by site-directed mutagenesis using complementary oligonucleotides bearing the nucleotide  
31 modifications. All constructs have been verified by restriction analysis and DNA sequencing  
32 (Eurofins, MWG).

33 **Bacterial two-hybrid assay.** The adenylate cyclase-based bacterial two-hybrid technique<sup>54</sup> was used  
34 as previously published.<sup>55</sup> Briefly, compatible vectors producing proteins fused to the isolated T18 and

1 T25 catalytic domains of the *Bordetella* adenylate cyclase were transformed into the reporter BTH101  
2 strain and the plates were incubated at 30°C for 24 hours. Three independent colonies for each  
3 transformation were inoculated into 600  $\mu$ L of LB medium supplemented with ampicillin, kanamycin  
4 and IPTG (0.5 mM). After overnight growth at 30°C, 10  $\mu$ L of each culture were spotted onto LB  
5 plates supplemented with ampicillin (100  $\mu$ g/mL), kanamycin (50  $\mu$ g/mL), IPTG (0.5 mM) and  
6 bromo-chloro-indolyl- $\beta$ -D-galactopyrannoside (40  $\mu$ g/mL) and incubated for 16 hours at 30 °C. The  
7 experiments were done at least in triplicate from independent transformations and a representative  
8 result is shown.

9 **Co-immunoprecipitations.** W3110 cells producing the protein of interest were grown to an  $A_{600} \sim 0.4$   
10 and the expression of the cloned genes were induced with AHT (0.1  $\mu$ g/mL) or L-arabinose (0.2%) for  
11 1 hour.  $10^{10}$  cells were harvested, and the pellets were resuspended in 1 mL of LyticB buffer (Sigma-  
12 Aldrich) supplemented with lysozyme 100  $\mu$ g/mL, DNase 100  $\mu$ g/mL and protease inhibitors  
13 (Complete, Roche) and incubated for 20 min at 25°C. Lysates were then clarified by centrifugation at  
14  $20,000 \times g$  for 10 min. 250  $\mu$ L of each lysate were mixed, incubated for 30 min on a wheel and the  
15 mixture was applied on anti-FLAG M2 affinity gel (Sigma-Aldrich). After 2 hours of incubation, the  
16 beads were washed three times with 1 mL of 20 mM Tris-HCl pH 7.5, 100 mM NaCl, resuspended in  
17 25  $\mu$ L of Laemmli loading buffer, boiled for 10 min and subjected to SDS-PAGE and  
18 immunodetection analyses.

19 **Anti-bacterial competition assay.** Antibacterial competition growth assays were performed as  
20 previously described in Sci-1-inducing conditions<sup>27</sup>, except that cultures were supplemented with  
21 IPTG 50  $\mu$ M, and that IPTG (10  $\mu$ M) was added on the competition plates. The wild-type *E. coli*  
22 strain W3110 bearing the kanamycin-resistant GFP<sup>+</sup> pUA66-*rrnB* plasmid<sup>51</sup> was used as prey. After  
23 incubation on plates for 4 hours, cells were scratched off and the fluorescence levels were measured  
24 using a TECAN infinite M200 microplate reader. The number of surviving prey cells was measured  
25 by counting fluorescent colonies on kanamycin plates.

26 **Protein purification.** The TssE protein and TssL cytoplasmic domain produced from pETG20A  
27 derivatives are fused to an N-terminal 6 $\times$ His-tagged thioredoxin (TRX) followed by a cleavage site for  
28 the Tobacco etch virus (TEV) protease. Purifications of TssE and TssL<sub>Cyto</sub> have been performed as  
29 previously described.<sup>42,45</sup> Briefly, *E. coli* BL21(DE3) pLysS cells carrying the pETG20A plasmid  
30 derivatives were grown at 37°C in TB medium (1.2% peptone, 2.4% yeast extract, 72 mM K<sub>2</sub>HPO<sub>4</sub>,  
31 17 mM KH<sub>2</sub>PO<sub>4</sub>, and 0.4% glycerol) and expression of the cloned genes was induced at  $A_{600} = 0.6$  with  
32 0.5 mM IPTG for 18 hours at 16°C. Cells were then resuspended in lysis buffer (50 mM Tris-HCl pH  
33 8.0, 300 mM NaCl, 1 mM EDTA, 0.5 mg/mL lysozyme, 1mM phenylmethylsulfonyl fluoride),  
34 submitted to four freeze-thawing cycles and sonicated after the addition of 20  $\mu$ g/mL DNase and 20

1 mM MgCl<sub>2</sub>. The soluble fraction obtained after centrifugation for 30 min at 16,000 × g was loaded onto a 5-mL Nickel column (HisTrap™ FF) using an ÄKTA Explorer apparatus (GE healthcare) and the immobilized proteins were eluted in 50 mM Tris-HCl pH8.0, 300 mM NaCl supplemented with 250 mM imidazole. The protein solution was desalted on a HiPrep 26/10 column (Sephadex™ G-25, Amersham Biosciences), and untagged proteins were obtained by cleavage using 2 mg of TEV protease for 18 hours at 4°C and collected in the flow-through of a 5-mL Nickel column. The proteins were concentrated using the centricon technology (Millipore, 10-kDa cut-off). After concentration, the soluble proteins were passed through a Sephadex 200 26/60 column pre-equilibrated with 25 mM Tris-HCl pH7.5, 100 mM NaCl, 5% Glycerol.

10 **Surface Plasmon Resonance (SPR).** Steady state interactions were monitored by SPR using a BIAcore T200 at 25°C, as previously described.<sup>39</sup> Briefly, the HC200m sensor chip (Xantech) was coated with purified the thioredoxin-TssE fusion protein immobilized by amine coupling ( $\Delta$ RU=4000-4300). A control flow-cell was coated with thioredoxin immobilized by amine coupling at the same concentration ( $\Delta$ RU=4100). Purified TssL<sub>Cyto</sub> (five concentrations ranging from 5 to 75  $\mu$ M) were injected and binding traces were recorded in duplicate. The signal from the control flow cell and the buffer response were subtracted from all measurements. The dissociation constants ( $K_D$ ) were estimated using the GraphPad Prism 5.0 software on the basis of the steady state levels of  $\Delta$ RU, directly related to the concentration of the analytes. The  $K_D$  were estimated by plotting the different  $\Delta$ RU at a fixed time (5 s before the end of the injection step) against the different concentrations of TssL<sub>Cyto</sub>. For  $K_D$  calculation, nonlinear regression fit for XY analysis was used and one site (specific binding) as a model which corresponds to the equation  $Y = B_{max} * X / (K_d + X)$ .

22

## 23 **References**

- 24 1. Coulthurst, S. J. (2013). The Type VI secretion system - a widespread and versatile cell targeting  
25 system. *Res Microbiol.* 164, 640-654.
- 26 2. Zoued, A., Brunet, Y. R., Durand, E., Aschtgen, M. S., Logger, L., Douzi, B., Journet, L.,  
27 Cambillau, C. & Cascales, E. (2014). Architecture and assembly of the Type VI secretion system.  
28 *Biochim Biophys Acta.* 1843, 1664-1673.
- 29 3. Durand, E., Cambillau, C., Cascales, E. & Journet, L. (2014). VgrG, Tae, Tle, and beyond: the  
30 versatile arsenal of Type VI secretion effectors. *Trends Microbiol.* 22, 498-507.
- 31 4. Ho, B. T., Dong, T. G. & Mekalanos, J. J. (2014). A view to a kill: the bacterial type VI secretion  
32 system. *Cell Host Microbe.* 15, 9-21.
- 33 5. Basler, M. (2015). Type VI secretion system: secretion by a contractile nanomachine. *Philos Trans*  
34 *R Soc Lond B Biol Sci.* 370, 1679.

- 1 6. Alcoforado Diniz, J., Liu, Y. C. & Coulthurst, S. J. (2015). Molecular weaponry: diverse effectors  
2 delivered by the Type VI secretion system. *Cell Microbiol.* 17, 1742-1751.
- 3 7. Basler, M., Pilhofer, M., Henderson, G. P., Jensen, G. J. & Mekalanos, J. J. (2012). Type VI  
4 secretion requires a dynamic contractile phage tail-like structure. *Nature.* 483, 182-186.
- 5 8. Cascales, E. & Cambillau, C. (2012). Structural biology of type VI secretion systems. *Philos Trans*  
6 *R Soc Lond B Biol Sci.* 367, 1102-1111.
- 7 9. Leiman, P. G., Basler, M., Ramagopal, U. A., Bonanno, J. B., Sauder, J. M., Pukatzki, S., Burley, S.  
8 K., Almo, S. C. & Mekalanos, J. J. (2009). Type VI secretion apparatus and phage tail-associated  
9 protein complexes share a common evolutionary origin. *Proc Natl Acad Sci USA.* 106, 4154-  
10 4159.
- 11 10. Bönemann, G., Pietrosiuk, A. & Mogk, A. (2010). Tubules and donuts: a type VI secretion story.  
12 *Mol Microbiol.* 76, 815-821.
- 13 11. Mougous, J. D., Cuff, M. E., Raunser, S., Shen, A., Zhou, M., Gifford, C. A., Goodman, A. L.,  
14 Joachimiak, G., Ordoñez, C. L., Lory, S., Walz, T., Joachimiak, A. & Mekalanos, J. J. (2006). A  
15 virulence locus of *Pseudomonas aeruginosa* encodes a protein secretion apparatus. *Science.* 312,  
16 1526-1530.
- 17 12. Ballister, E. R., Lai, A. H., Zuckermann, R. N., Cheng, Y. & Mougous, J. D. (2008). In vitro self-  
18 assembly of tailorable nanotubes from a simple protein building block. *Proc Natl Acad Sci USA.*  
19 105, 3733-3738.
- 20 13. Lossi, N. S., Manoli, E., Förster, A., Dajani, R., Pape, T., Freemont, P. & Filloux, A. (2013). The  
21 HsiB1C1 (TssB-TssC) complex of the *Pseudomonas aeruginosa* type VI secretion system forms a  
22 bacteriophage tail sheathlike structure. *J Biol Chem.* 288, 7536-7548.
- 23 14. Brunet, Y. R., Hénin, J., Celia, H. & Cascales, E. (2014). Type VI secretion and bacteriophage tail  
24 tubes share a common assembly pathway. *EMBO Rep.* 15, 315-321.
- 25 15. Douzi, B., Spinelli, S., Blangy, S., Roussel, A., Durand, E., Brunet, Y. R., Cascales, E. &  
26 Cambillau, C. (2014). Crystal structure and self-interaction of the type VI secretion tail-tube  
27 protein from enteroaggregative *Escherichia coli*. *PLoS One.* 9, e86918.
- 28 16. Zhang, X. Y., Brunet, Y. R., Logger, L., Douzi, B., Cambillau, C., Journet, L. & Cascales, E.  
29 (2013). Dissection of the TssB-TssC interface during type VI secretion sheath complex  
30 formation. *PLoS One.* 8, e81074.
- 31 17. Kudryashev, M., Wang, R. Y., Brackmann, M., Scherer, S., Maier, T., Baker, D., DiMaio, F.,  
32 Stahlberg, H., Egelman, E. H. & Basler, M. (2015). Structure of the type VI secretion system  
33 contractile sheath. *Cell.* 160, 952-962.
- 34 18. LeRoux, M., De Leon, J. A., Kuwada, N. J., Russell, A. B., Pinto-Santini, D., Hood, R. D.,  
35 Agnello, D. M., Robertson, S. M., Wiggins, P. A. & Mougous, J. D. (2012). Quantitative single-  
36 cell characterization of bacterial interactions reveals type VI secretion is a double-edged sword.  
37 *Proc Natl Acad Sci USA.* 109, 19804-19809.
- 38 19. Basler, M., Ho, B. T. & Mekalanos, J. J. (2013). Tit-for-tat: type VI secretion system counterattack  
39 during bacterial cell-cell interactions. *Cell.* 152, 884-894.

- 1 20. Brunet, Y. R., Espinosa, L., Harchouni, S., Mignot, T. & Cascales, E. (2013). Imaging type VI  
2 secretion-mediated bacterial killing. *Cell Rep.* 3, 36-41.
- 3 21. Shneider, M. M., Buth, S. A., Ho, B. T., Basler, M., Mekalanos, J. J. & Leiman, P. G. (2013).  
4 PAAR-repeat proteins sharpen and diversify the type VI secretion system spike. *Nature.* 500,  
5 350-353.
- 6 22. Pukatzki, S., Ma, A. T., Revel, A. T., Sturtevant, D. & Mekalanos, J. J. (2007). Type VI secretion  
7 system translocates a phage tail spike-like protein into target cells where it cross-links actin. *Proc*  
8 *Natl Acad Sci USA.* 104, 15508-15513.
- 9 23. Silverman, J. M., Agnello, D. M., Zheng, H., Andrews, B. T., Li, M., Catalano, C. E., Gonen, T. &  
10 Mougous, J. D. (2013). Haemolysin coregulated protein is an exported receptor and chaperone of  
11 type VI secretion substrates. *Mol Cell.* 51, 584-593.
- 12 24. Alcoforado Diniz, J., Liu, Y. C. & Coulthurst, S. J. (2015). Molecular weaponry: diverse effectors  
13 delivered by the Type VI secretion system. *Cell Microbiol.* 17, 1742-1751.
- 14 25. Unterweger, D., Kostiuk, B., Ötjengerdes, R., Wilton, A., Diaz-Satizabal, L. & Pukatzki, S.  
15 (2015). Chimeric adaptor proteins translocate diverse type VI secretion system effectors in *Vibrio*  
16 *cholerae*. *EMBO J.* 34, 2198-2210.
- 17 26. Liang, X., Moore, R., Wilton, M., Wong, M. J., Lam, L. & Dong, T. G. (2016). Identification of  
18 divergent type VI secretion effectors using a conserved chaperone domain. *Proc Natl Acad Sci*  
19 *USA.* 112, 9106-9111.
- 20 27. Flaugnatti, N., Le, T. T., Canaan, S., Aschtgen, M. S., Nguyen, V. S., Blangy, S., Kellenberger, C.,  
21 Roussel, A., Cambillau, C., Cascales, E. & Journet, L. (2016). A phospholipase A1 anti-bacterial  
22 T6SS effector interacts directly with the C-terminal domain of the VgrG spike protein for  
23 delivery. *Mol Microbiol.* 99, 1099-1118.
- 24 28. Bondage, D. D., Lin, J. S., Ma, L. S., Kuo, C. H. & Lai, E. M. (2016). VgrG C terminus confers  
25 the type VI effector transport specificity and is required for binding with PAAR and adaptor-  
26 effector complex. *Proc Natl Acad Sci USA.* 113, 3931-3940.
- 27 29. Cianfanelli, F. R., Alcoforado Diniz, J., Guo, M., De Cesare, V., Trost, M. & Coulthurst, S. J.  
28 (2016). VgrG and PAAR proteins define distinct versions of a functional Type VI secretion  
29 system. *PLoS Pathog.* 12, e1005735.
- 30 30. Leiman, P. G. & Shneider, M. M. (2012). Contractile tail machines of bacteriophages. *Adv Exp*  
31 *Med Biol.* 726, 93-114.
- 32 31. Sarris, P. F., Ladoukakis, E. D., Panopoulos, N. J. & Scoulica, E. V. (2014). A phage tail-derived  
33 element with wide distribution among both prokaryotic domains: a comparative genomic and  
34 phylogenetic study. *Genome Biol Evol.* 6, 1739-1747.
- 35 32. Brunet, Y. R., Zoued, A., Boyer, F., Douzi, B. & Cascales, E. (2015). The Type VI secretion  
36 TssEFGK-VgrG phage-like baseplate is recruited to the TssJLM membrane complex via multiple  
37 contacts and serves as assembly platform for tail tube/sheath polymerization. *PLoS Genet.* 11,  
38 e1005545.
- 39 33. Taylor, N. M., Prokhorov, N. S., Guerrero-Ferreira, R. C., Shneider, M. M., Browning, C., Goldie,  
40 K. N., Stahlberg, H. & Leiman, P. G. (2016). Structure of the T4 baseplate and its function in

- 1 triggering sheath contraction. *Nature*. 533, 346-352.
- 2 34. Filloux, A. & Freemont, P. (2016). Structural biology: baseplates in contractile machines. *Nat*  
3 *Microbiol.* in press.
- 4 35. English, G., Byron, O., Cianfanelli, F. R., Prescott, A. R. & Coulthurst, S. J. (2014). Biochemical  
5 analysis of TssK, a core component of the bacterial Type VI secretion system, reveals distinct  
6 oligomeric states of TssK and identifies a TssK-TssFG subcomplex. *Biochem J.* 461, 291-304.
- 7 36. Aschtgen, M. S., Gavioli, M., Dessen, A., Lloubès, R. & Cascales, E. (2010). The SciZ protein  
8 anchors the enteroaggregative *Escherichia coli* Type VI secretion system to the cell wall. *Mol*  
9 *Microbiol.* 75, 886-899.
- 10 37. Durand, E., Nguyen, V. S., Zoued, A., Logger, L., Péhau-Arnaudet, G., Aschtgen, M. S., Spinelli,  
11 S., Desmyter, A., Bardiaux, B., Dujeancourt, A., Roussel, A., Cambillau, C., Cascales, E. &  
12 Fronzes, R. (2015). Biogenesis and structure of a type VI secretion membrane core complex.  
13 *Nature*. 523, 555-560.
- 14 38. Aschtgen, M. S., Bernard, C. S., De Bentzmann, S., Lloubès, R. & Cascales, E. (2008). SciN is an  
15 outer membrane lipoprotein required for type VI secretion in enteroaggregative *Escherichia coli*.  
16 *J Bacteriol.* 190, 7523-7531.
- 17 39. Felisberto-Rodrigues, C., Durand, E., Aschtgen, M. S., Blangy, S., Ortiz-Lombardia, M., Douzi,  
18 B., Cambillau, C. & Cascales, E. (2011). Towards a structural comprehension of bacterial type VI  
19 secretion systems: characterization of the TssJ-TssM complex of an *Escherichia coli* pathovar.  
20 *PLoS Pathog.* 7, e1002386.
- 21 40. Ma, L. S., Lin, J. S. & Lai, E. M. (2009). An IcmF family protein, ImpLM, is an integral inner  
22 membrane protein interacting with ImpKL, and its walker a motif is required for type VI  
23 secretion system-mediated Hcp secretion in *Agrobacterium tumefaciens*. *J Bacteriol.* 191, 4316-  
24 4129.
- 25 41. Aschtgen, M. S., Zoued, A., Lloubès, R., Journet, L. & Cascales, E. (2012). The C-tail anchored  
26 TssL subunit, an essential protein of the enteroaggregative *Escherichia coli* Sci-1 Type VI  
27 secretion system, is inserted by YidC. *Microbiologyopen.* 1, 71-82.
- 28 42. Durand, E., Zoued, A., Spinelli, S., Watson, P. J., Aschtgen, M. S., Journet, L., Cambillau, C. &  
29 Cascales, E. (2012). Structural characterization and oligomerization of the TssL protein, a  
30 component shared by bacterial type VI and type IVb secretion systems. *J Biol Chem.* 287, 14157-  
31 14168.
- 32 43. Robb, C. S., Nano, F. E. & Boraston, A. B. (2012). The structure of the conserved type six  
33 secretion protein TssL (DotU) from *Francisella novicida*. *J Mol Biol.* 419, 277-283.
- 34 44. Chang, J. H. & Kim, Y. G. (2015). Crystal structure of the bacterial type VI secretion system  
35 component TssL from *Vibrio cholerae*. *J Microbiol.* 53, 32-37.
- 36 45. Zoued, A., Durand, E., Brunet, Y. R., Spinelli, S., Douzi, B., Guzzo, M., Flaugnatti, N., Legrand,  
37 P., Journet, L., Fronzes, R., Mignot, T., Cambillau, C. & Cascales, E. (2016). Priming and  
38 polymerization of a bacterial contractile tail structure. *Nature*. 531, 59-63.
- 39 46. Zoued, A., Durand, E., Bebeacua, C., Brunet, Y. R., Douzi, B., Cambillau, C., Cascales, E. &  
40 Journet, L. (2013). TssK is a trimeric cytoplasmic protein interacting with components of both

- 1 phage-like and membrane anchoring complexes of the type VI secretion system. *J Biol Chem.*  
2 288, 27031-27041.
- 3 47. Logger, L., Aschtgen, M. S., Guérin, M., Cascales, E. & Durand, E. (2016). Molecular dissection  
4 of the interface between the Type VI secretion TssM cytoplasmic domain and the TssG baseplate  
5 component. *J Mol Biol*
- 6 48. Gerc, A. J., Diepold, A., Trunk, K., Porter, M., Rickman, C., Armitage, J. P., Stanley-Wall, N. R.  
7 & Coulthurst, S. J. (2015). Visualization of the *Serratia* Type VI secretion system reveals  
8 unprovoked attacks and dynamic assembly. *Cell Rep.* 12, 2131-2142.
- 9 49. Kostyuchenko, V. A., Leiman, P. G., Chipman, P. R., Kanamaru, S., van Raaij, M. J., Arisaka, F.,  
10 Mesyanzhinov, V. V. & Rossmann, M. G. (2003). Three-dimensional structure of bacteriophage  
11 T4 baseplate. *Nat Struct Biol.* 10, 688-693.
- 12 50. Gueguen, E. & Cascales, E. (2013). Promoter swapping unveils the role of the *Citrobacter*  
13 *rodentium* CTS1 type VI secretion system in interbacterial competition. *Appl Environ Microbiol.*  
14 79, 32-38.
- 15 51. Zaslaver, A., Bren, A., Ronen, M., Itzkovitz, S., Kikoin, I., Shavit, S., Liebermeister, W., Surette,  
16 M. G. & Alon, U. (2006). A comprehensive library of fluorescent transcriptional reporters for  
17 *Escherichia coli*. *Nat Methods.* 3, 623-628.
- 18 52. Brunet, Y. R., Bernard, C. S., Gavioli, M., Llobès, R. & Cascales, E. (2011). An epigenetic  
19 switch involving overlapping *fur* and DNA methylation optimizes expression of a type VI  
20 secretion gene cluster. *PLoS Genet.* 7, e1002205.
- 21 53. van den Ent, F. & Löwe, J. (2006). RF cloning: a restriction-free method for inserting target genes  
22 into plasmids. *J Biochem Biophys Methods.* 67, 67-74.
- 23 54. Karimova, G., Pidoux, J., Ullmann, A. & Ladant, D. (1998). A bacterial two-hybrid system based  
24 on a reconstituted signal transduction pathway. *Proc Natl Acad Sci USA.* 95, 5752-5756.
- 25 55. Battesti, A. & Bouveret, E. (2012). The bacterial two-hybrid system based on adenylate cyclase  
26 reconstitution in *Escherichia coli*. *Methods.* 58, 325-334.
- 27 56. Pettersen, E. F., Goddard, T. D., Huang, C. C., Couch, G. S., Greenblatt, D. M., Meng, E. C. &  
28 Ferrin, T. E. (2004). UCSF Chimera - a visualization system for exploratory research and  
29 analysis. *J Comput Chem.* 25, 1605-1612.

30

## 31 **Acknowledgements**

32 We thank Laetitia Houot and Bérengère Ize and the members of the Cascales,  
33 Cambillau, Llobès, Bouveret and Sturgis research groups for insightful discussions, Annick  
34 Brun, Isabelle Bringer and Olivier Uderso for technical assistance, and Marc Assin for  
35 encouragements. This work was supported by the Centre Nationale de la Recherche  
36 Scientifique (CNRS), the Aix-Marseille Université (AMU) and Agence Nationale de la  
37 Recherche (ANR) and Fondation pour la Recherche Médicale (FRM) research grants (ANR-

1 10-JCJC-1303-03, ANR-14-CE14-0006-02, DEQ2011-0421282). A.Z. was a recipient of a  
2 Ministère de la Recherche doctoral and FRM end-of-thesis (FDT20140931060) fellowships.

3

#### 4 **Authors contribution**

5 A.Z., A.E. and L.J. constructed the vectors for the *in vivo* studies and performed the BACTH  
6 experiments, Chl.C. performed the co-immunoprecipitations and anti-bacterial assays, A.Z.,  
7 E.D. and E.C. analysed the TssL structure and identified regions for mutagenesis, B.D.  
8 purified TssE and performed SPR experiments E.C. and C.C. supervised the experiments.  
9 E.C. wrote the manuscript. Each author reviewed the manuscript prior to submission.

#### 10 **Additional information**

11 **Supplemental information.** The supplemental information contains one Supplemental Table  
12 (Strains, Plasmids and Oligonucleotides used in this study) and two Supplemental Figure (S1,  
13 Comparison of the EAEC, *F. tularensis* and *V. cholerae* TssL<sub>Cyto</sub> structures; S2, Sequence  
14 alignment of TssL proteins).

15 **Competing financial interests.** The authors declare no competing financial interests.

## 1 Legend to Figures

2 **Figure 1. TssL<sub>Cyto</sub> oligomerizes and interacts with TssE, TssK and TssM<sub>Cyto</sub>.** (A) Bacterial two-  
3 hybrid assay. BTH101 reporter cells producing the TssL<sub>Cyto</sub>-T18 fusion protein and the indicated T6SS  
4 proteins fused to the T25 domain of the *Bordetella* adenylate cyclase were spotted on X-Gal-IPTG  
5 reporter LB agar plates. Only the cytoplasmic (Cyto) or periplasmic (Peri) domains were used for  
6 membrane-anchored proteins. (B and C) Surface plasmon resonance analysis. SPR sensorgrams  
7 (expressed as variation of resonance units,  $\Delta$ RU) were recorded after injection of the increasing  
8 concentrations of purified TssL<sub>Cyto</sub> (from light grey to black: 5, 10, 20, 37.5 and 75  $\mu$ M) on TssE-  
9 coated HC200m chips (B). The graphs reporting  $\Delta$ RU as a function of TssL<sub>Cyto</sub> concentration were  
10 used to estimate the dissociation constants of the TssL<sub>Cyto</sub>-TssE complex (C).

11 **Figure 2. Structure of the EAEC TssL<sub>Cyto</sub> domain.** (A) Crystal structure of the EAEC TssL<sub>Cyto</sub>  
12 domain. The protein is shown as ribbon and  $\alpha$ -helices ( $\alpha$ 1- $\alpha$ 7) are indicated. The unstructured L3-L4  
13 loop (orange arrow) is shown in dotted line, whereas the L6-L7 loop and the cleft are indicated by blue  
14 and green arrows respectively. The figure was made with Chimera.<sup>56</sup> (B) Sequence of the crystallized  
15 TssL<sub>Cyto</sub> domain, with the same color code that in panel A. The residues substituted in this study are  
16 indicated by arrowheads (green, cleft; orange, L3-L4 loop; blue, L6-L7 loop).

17 **Figure 3. Distinct motifs on TssL<sub>Cyto</sub> mediate interactions with TssE, TssK and TssM<sub>Cyto</sub>** (A)  
18 Bacterial two-hybrid assay. BTH101 reporter cells producing the TssL<sub>Cyto</sub>-T18 fusion protein variants  
19 and the indicated T6SS proteins fused to the T25 domain of the *Bordetella* adenylate cyclase were  
20 spotted on X-Gal-IPTG reporter LB agar plates. Only the cytoplasmic (*c*) or periplasmic (*p*) domains  
21 were used for membrane-anchored proteins. (B) Co-immunoprecipitation assay. Soluble lysates from  
22  $3 \times 10^{10}$  *E. coli* K12 W3110 cells producing WT or mutant FLAG-tagged TssL<sub>Cyto</sub> (Lc<sub>FL</sub>) and VSV-G-  
23 tagged TssE (TssE<sub>V</sub>), TssK (TssK<sub>V</sub>) or TssM<sub>Cyto</sub> (TssMc<sub>V</sub>) proteins were subjected to  
24 immunoprecipitation with anti-FLAG-coupled beads. The lysates and immunoprecipitated (IP)  
25 material were separated by 12.5% acrylamide SDS-PAGE and immunodetected with anti-FLAG  
26 (lower panels) and anti-VSV-G (upper panels) monoclonal antibodies. Molecular weight markers (in  
27 kDa) are indicated.

28 **Figure 4. TssL<sub>Cyto</sub> interactions with TssE, TssK and TssM<sub>Cyto</sub> are required for T6SS anti-**  
29 **bacterial activity.** *E. coli* K-12 prey cells (W3110 *gfp*<sup>+</sup>, kan<sup>R</sup>) were mixed with the indicated attacker  
30 cells, spotted onto Sci-1 inducing medium (SIM) agar plates and incubated for 4 hours at 37°C. The  
31 relative fluorescence of the bacterial mixture (in arbitrary unit, AU) is indicated in the upper graph,  
32 and the number of recovered *E. coli* prey cells (counted on selective kanamycin medium) is indicated  
33 in the graph (in log<sub>10</sub> of colony-forming unit (cfu)). The circles indicate values from three

1 independent assays, and the average is indicated by the bar.

2 **Figure 5. Schematic representation of the TssL<sub>Cyto</sub> interaction network.** Schematic representation  
3 of the TssJLM membrane complex (MC) and its interactions with the TssKEFG-VgrG baseplate  
4 complex (BC). The TssL (TssL<sub>Cyto</sub>) and TssM (TssM<sub>Cyto</sub>) cytoplasmic domains are shown in orange  
5 and blue respectively. The interactions defined in this study are indicated by red arrows. Interactions  
6 determined previously<sup>46</sup> or in the accompanying article<sup>47</sup> are shown in blue dashed arrows.

7

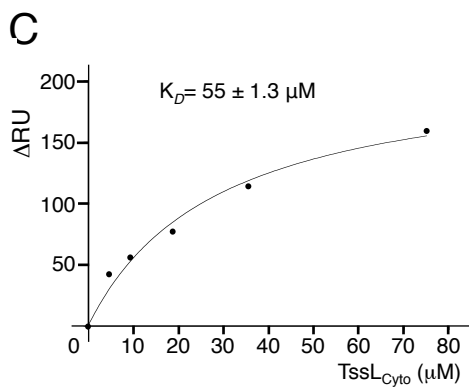
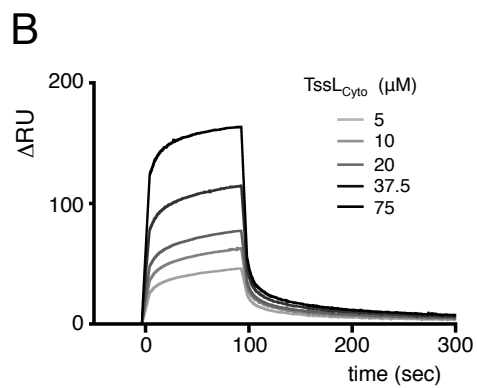
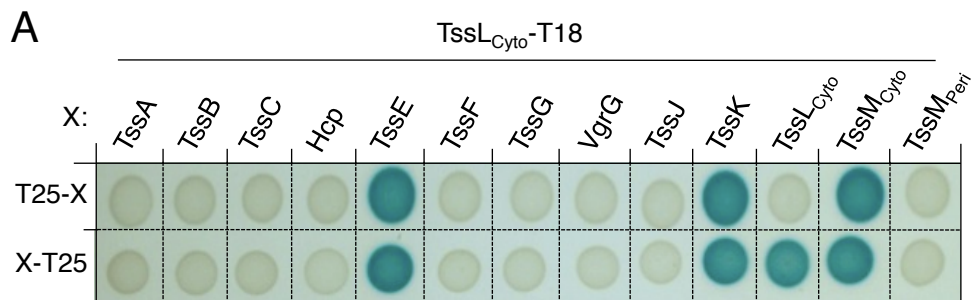
## 8 **Legend to Supplementary Data**

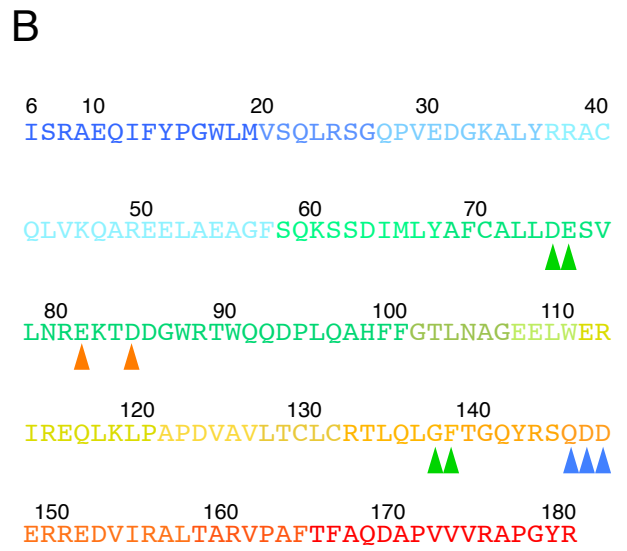
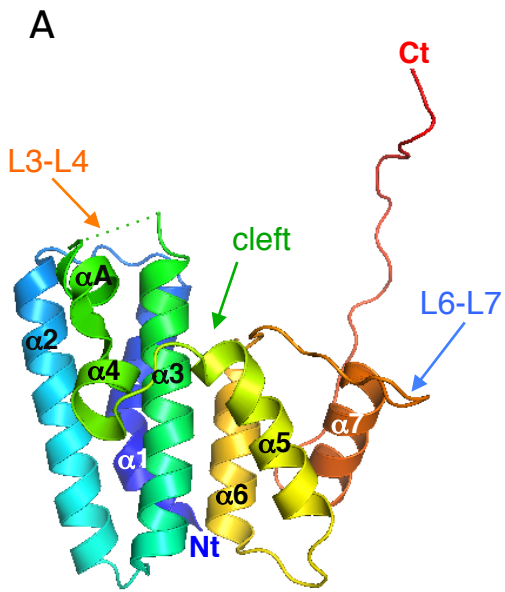
9 **Figure S1. Comparison of the three available TssL<sub>Cyto</sub> crystal structures.** (A) Sequence alignment  
10 of the enteroaggregative *E. coli* (EAEC), *Francisella* and *Vibrio* TssL<sub>Cyto</sub> sequences. The secondary  
11 structures of the EAEC TssL<sub>Cyto</sub> protein are shown on top whereas conserved residues are shown in  
12 red. The residues substituted in this study are indicated by arrowheads (green, cleft; orange, L3-L4  
13 loop; blue, L6-L7 loop). (B) Merged crystal structures of the EAEC (PDB: 3U66; green), *Francisella*  
14 *tularensis* (PDB: 4ACL, purple) and *Vibrio cholerae* (PDB: 3V3I, blue) TssL<sub>Cyto</sub> domains. The  
15 positions of the cleft, L3-L4 and L6-L7 loops are indicated by green, orange and blue arrows. (C-E)  
16 Crystal structures of EAEC (PDB: 3U66; C), *Francisella tularensis* (PDB: 4ACL, D) and *Vibrio*  
17 *cholerae* (PDB: 3V3I, E) TssL<sub>Cyto</sub> domains. Panel C highlights the positions and locations of the  
18 residues substituted, as well as helix  $\alpha$ A (loop L3-L4) whereas panel E highlights helices  $\alpha$ A (loop  
19 L3-L4) and  $\alpha$ B (loop L6-L7). The figures were made with Chimera.<sup>56</sup>

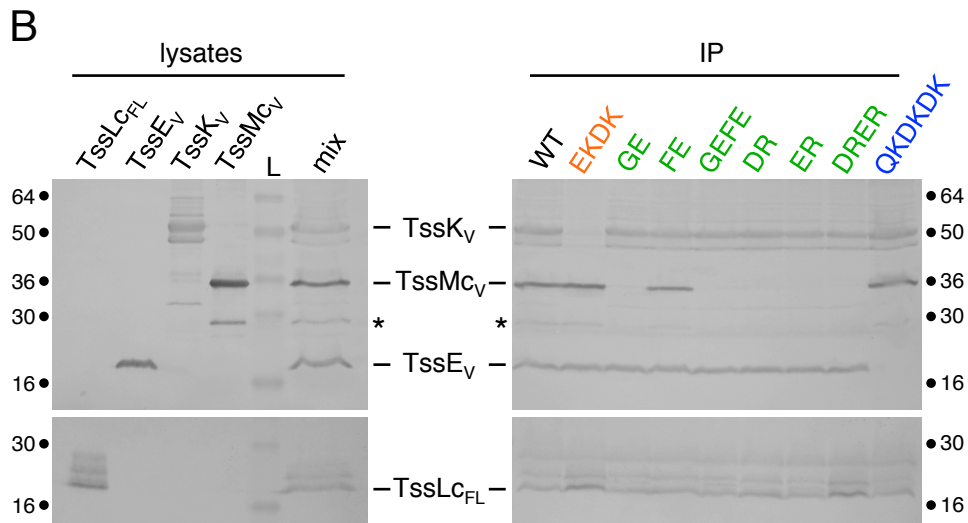
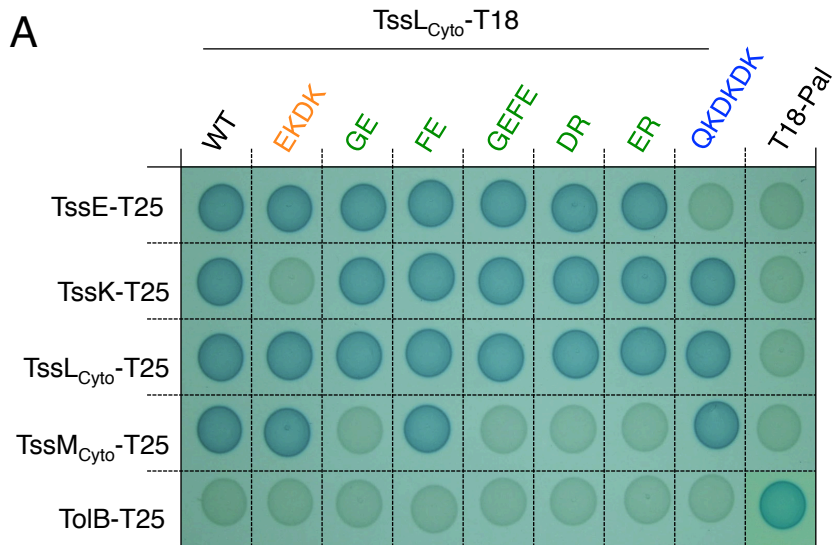
20

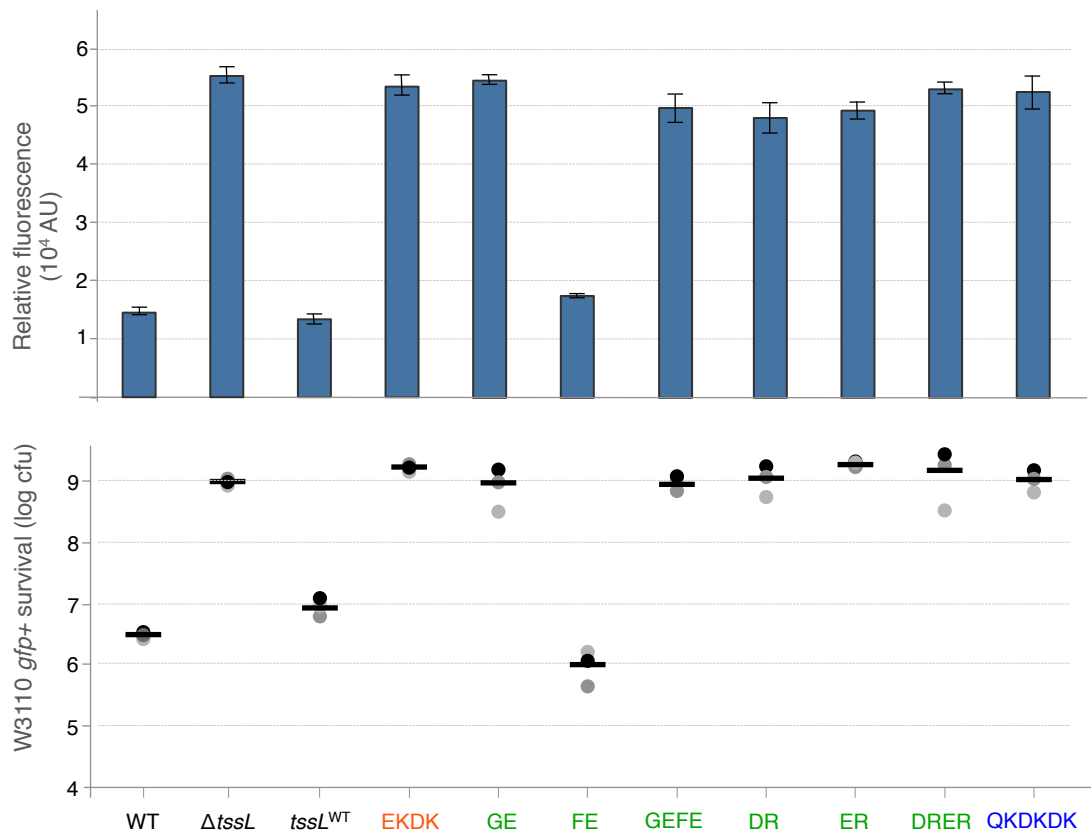
21 **Table S1. Strains, Plasmids and Oligonucleotides used in this study.**

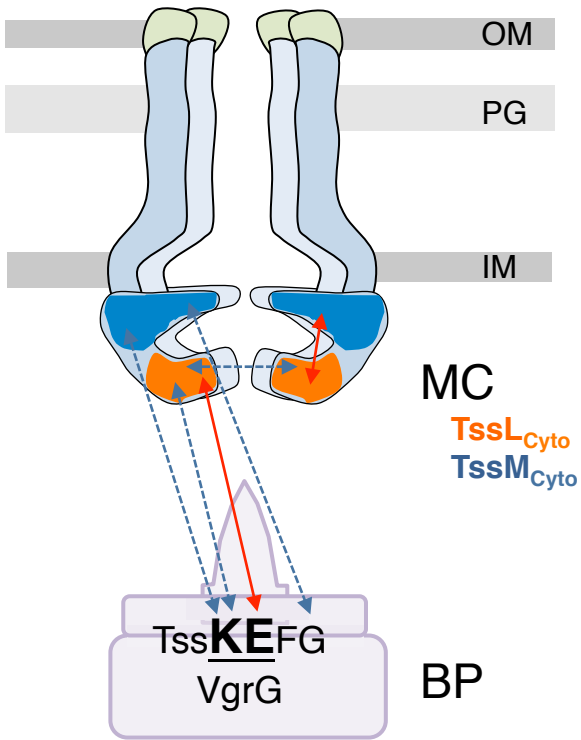
22











## **SUPPLEMENTAL DATA**

**Structure-function analysis of the TssL cytoplasmic domain reveals a new interaction between the Type VI secretion baseplate and membrane complexes.**

A. Zoued, C.J. Cassaro, E. Durand, B. Douzi, A.P. España, C. Cambillau, L. Journet, & E. Cascales

## Supplemental Table S1. Strains, plasmids and oligonucleotides used in this study.

### Strains

Strains	Description and genotype	Source
<i>E. coli</i> K-12		
DH5 $\alpha$	F-, $\Delta$ ( <i>argF-lac</i> )U169, <i>phoA</i> , <i>supE44</i> , $\Delta$ ( <i>lacZ</i> )M15, <i>relA</i> , <i>endA</i> , <i>thi</i> , <i>hsdR</i>	New England Biolabs
W3110	F-, lambda- IN( <i>rrnD-rrnE</i> )1 <i>rph-1</i>	Laboratory collection
BTH101	F-, <i>cya-99</i> , <i>araD139</i> , <i>galE15</i> , <i>galK16</i> , <i>rpsL1</i> ( <i>Str<sup>R</sup></i> ), <i>hsdR2</i> , <i>mcrA1</i> , <i>mcrB1</i> .	Karimova <i>et al.</i> , 2005
BL21(DE3) pLys	F-, miniF <i>lysY lacI<sup>f</sup></i> (Cm <sup>R</sup> ) / <i>fhuA2 lacZ::T7 gene1 [lon] ompT gal sulA11 R(mcr-73::miniTn10--Tet<sup>S</sup>)2 [dcm] R(zgb-210::Tn10-Tet<sup>S</sup>) endA1 <math>\Delta</math>(<i>mcrC-mrr</i>) 114::IS10</i>	New England Biolabs
Enterogaagregative <i>E. coli</i>		
17-2	WT enterogaagregative <i>Escherichia coli</i>	Arlette Darfeuille-Michaud
17-2 $\Delta$ <i>tssL</i>	17-2 deleted of the <i>tssL</i> gene of the <i>sci1</i> T6SS gene cluster (EC042_4527)	Aschtgen <i>et al.</i> , 2010

### Plasmids

Vectors	Description	Source
Expression vectors		
pUA66- <i>rrnB</i>	<i>P<sub>rrnB</sub></i> :: <i>gfpmut2</i> transcriptional fusion in pUA66	Zaslaver <i>et al.</i> , 2006
pMS600	cloning vector, pOK12 derivative, P15A origin, <i>Plac</i> , Kan <sup>R</sup>	Aschtgen <i>et al.</i> , 2008
pOK-TssL <sub>HA</sub>	<i>sci1 tssL</i> (EC042_4527), C-terminal HA tag cloned into pMS600	Aschtgen <i>et al.</i> , 2010
pOK-TssL-EKDK	Glu81-to Lys and Asp84-to-Lys substitutions introduced into pOK-TssL <sub>HA</sub>	This study
pOK-TssL-GE	Gly137-to-Glu substitution introduced into pOK-TssL <sub>HA</sub>	This study
pOK-TssL-FE	Phe138-to-Glu substitution introduced into pOK-TssL <sub>HA</sub>	This study

pOK-TssL-GEFE	Gly137-to-Glu and Phe138-to-Glu substitutions introduced into pOK-TssL <sub>HA</sub>	This study
pOK-TssL-DR	Asp74-to-Arg substitution introduced into pOK-TssL <sub>HA</sub>	This study
pOK-TssL-ER	Glu75-to-Arg substitution introduced into pOK-TssL <sub>HA</sub>	This study
pOK-TssL-DRER	Asp74-to-Arg and Glu75-to-Arg substitutions introduced into pOK-TssL <sub>HA</sub>	This study
pOK-TssL-QKDKDK	Gln145-to-Lys, Asp146-to-Lys and Asp147-to-Lys substitutions introduced into pOK-TssL <sub>HA</sub>	This study
pASK-IBA37(+)	cloning vector, fl origin, <i>Ptet</i> , Amp <sup>R</sup>	IBA technologies
pIBA-TssL <sub>CFL</sub>	<i>scil tssL</i> cytoplasmic domain (amino-acids 1-184; TssL <sub>Cyto</sub> ), C-terminal FLAG tag cloned into pASK-IBA37(+)	Aschtgen <i>et al.</i> , 2012
pIBA-TssL <sub>C</sub> -EKDK	Glu81-to-Lys and Asp84-to-Lys substitutions introduced into pIBA-TssL <sub>CFL</sub>	This study
pIBA-TssL <sub>C</sub> -GE	Gly137-to-Glu substitution introduced into pIBA-TssL <sub>CFL</sub>	This study
pIBA-TssL <sub>C</sub> -FE	Phe138-to-Glu substitution introduced into pIBA-TssL <sub>CFL</sub>	This study
pIBA-TssL <sub>C</sub> -GEFE	Gly137-to-Glu and Phe138-to-Glu substitutions introduced into pIBA-TssL <sub>CFL</sub>	This study
pIBA-TssL <sub>C</sub> -DR	Asp74-to-Arg substitution introduced into pIBA-TssL <sub>CFL</sub>	This study
pIBA-TssL <sub>C</sub> -ER	Glu75-to-Arg substitution introduced into pIBA-TssL <sub>CFL</sub>	This study
pIBA-TssL <sub>C</sub> -DRER	Asp74-to-Arg and Glu75-to-Arg substitutions introduced into pIBA-TssL <sub>CFL</sub>	This study
pIBA-TssL <sub>C</sub> -QKDKDK	Gln145-to-Lys, Asp146-to-Lys and Asp147-to-Lys substitutions introduced into pIBA-TssL <sub>CFL</sub>	This study
pBAD33	cloning vector, P15A origin, <i>Para</i> , <i>araC</i> Cm <sup>R</sup>	Guzman <i>et al.</i> , 1995
pBAD33-TssE <sub>VSV-G</sub>	<i>scil tssE</i> (EC042_4545), C-terminal VSV-G tag cloned into pBAD33	This study
pBAD33-TssK <sub>VSV-G</sub>	<i>scil tssK</i> (EC042_4526), C-terminal VSV-G tag cloned into pBAD33	This study
pBAD33-TssM <sub>VSV-G</sub>	<i>scil tssM</i> (EC042_4539) cytoplasmic loop (amino-acids 62-360, TssM <sub>Cyto</sub> ), C-terminal VSV-G tag cloned into pBAD33	Lauren Logger
pETG20A	Gateway <sup>®</sup> expression vector, ColE1 origin, <i>P<sub>T7</sub></i> , N-terminal 6xHis-TRX-TEV fusion, Amp <sup>R</sup>	Arie Geerlof
pETG20A-TssL <sub>Cyto</sub>	<i>scil tssL</i> cytoplasmic domain (amino-acids 1-184) cloned into pETG20A	Durand <i>et al.</i> , 2012
pETG20A-TssE	<i>scil tssE</i> cloned into pETG20A	Zoued <i>et al.</i> , 2016

### Bacterial Two-Hybrid vectors

pT18-FLAG	Bacterial two-hybrid vector, ColE1 origin, <i>Plac</i> , T18 fragment of <i>Bordetella pertussis</i> CyaA, Amp <sup>R</sup>	Battesti & Bouveret, 2008
pT18-Pal	Soluble region of <i>E. coli</i> K-12 Pal cloned downstream T18 in pT18-FLAG	Battesti & Bouveret, 2008
pTssL <sub>C</sub> -T18	<i>scil tssL</i> cytoplasmic domain (amino-acids 1-184) cloned upstream T18 into pT18-FLAG	Durand <i>et al.</i> , 2012
pTssL <sub>C</sub> -EKDK-T18	Glu81-to-Lys and Asp84-to-Lys substitutions introduced into pTssL <sub>C</sub> -T18	This study
pTssL <sub>C</sub> -GE-T18	Gly137-to-Glu substitution introduced into pTssL <sub>C</sub> -T18	This study
pTssL <sub>C</sub> -FE-T18	Phe138-to-Glu substitution introduced into pTssL <sub>C</sub> -T18	This study
pTssL <sub>C</sub> -GEFE-T18	Gly137-to-Glu and Phe138-to-Glu substitutions introduced into pTssL <sub>C</sub> -T18	This study
pTssL <sub>C</sub> -DR-T18	Asp74-to-Arg substitution introduced into pTssL <sub>C</sub> -T18	This study
pTssL <sub>C</sub> -ER-T18	Glu75-to-Arg substitution introduced into pTssL <sub>C</sub> -T18	This study
pTssL <sub>C</sub> -DRER-T18	Asp74-to-Arg and Glu75-to-Arg substitutions introduced into pTssL <sub>C</sub> -T18	This study
pTssL <sub>C</sub> -QKDKDK-T18	Gln145-to-Lys, Asp146-to-Lys and Asp147-to-Lys substitutions introduced into pTssL <sub>C</sub> -T18	This study
pT25-FLAG	Bacterial two-hybrid vector, P15A origin, <i>Plac</i> , T25 fragment of <i>Bordetella pertussis</i> CyaA, Kan <sup>R</sup>	Battesti & Bouveret, 2008

All others BACTH constructs have been described in Zoued *et al.*, 2013.

## Oligonucleotides

Name	Sequence (5' to 3')
For site-directed mutagenesis <sup>a</sup>	
A-TssL-EKDK	ACGAGAGTGTACTGAACCGCAAAAAAAAACAAAGGATGGCTGGCGCACCTGGC
B-TssL-EKDK	GCCAGGTGCGCCAGCCATCCTTTGTTTTTTTGGCGTTCAGTACACTCTCGTC
A-TssL-GE	CTCTGCCGTACGCTTCAGCTCGAGTTTACCGGTCAGTACCGGTCGCAG
B-TssL-GE	CTGCGACCGGTACTGACCGGTAAACTCGAGCTGAAGCGTACGGCAGAG
A-TssL-FE	CTCTGCCGTACGCTTCAGCTCGGTGAGACCGGTCAGTACCGGTCGCAG
B-TssL-FE	CTGCGACCGGTACTGACCGGTCTCACCAGCTGAAGCGTACGGCAGAG
A-TssL-GEFE	CTCTGCCGTACGCTTCAGCTCGAGGAGACCGGTCAGTACCGGTCGCAG
B-TssL-GEFE	CTGCGACCGGTACTGACCGGTCTCCTCGAGCTGAAGCGTACGGCAGAG
A-TssL-DR	GTATGCCTTCTGCGCCCTGCTGCGCGAGAGTGTACTGAACCGCGAAAAAAC
B-TssL-DR	GTTTTTTCGCGTTCAGTACACTCTCGCGCAGCAGGGCGCAGAAGGCATAC
A-TssL-ER	GTATGCCTTCTGCGCCCTGCTGGACCGGAGTGTACTGAACCGCGAAAAAAC
B-TssL-ER	GTTTTTTCGCGTTCAGTACACTCCGGTCCAGCAGGGCGCAGAAGGCATAC
A-TssL-DRER	GTATGCCTTCTGCGCCCTGCTGCGCCGGAGTGTACTGAACCGCGAAAAAAC
B-TssL-DRER	GTTTTTTCGCGTTCAGTACACTCCGGCGCAGCAGGGCGCAGAAGGCATAC
A-TssL-QKDKDK	TTACCGGTCAGTACCGGTCGAAAGAAAAAGGAGCGTCGCGAAGATGTAATAC
B-TssL-QKDKDK	GTATTACATCTTCGCGACGCTCCTTTTTCTTCGACCGGTACTGACCGGTAAAAAC

<sup>a</sup> Mutagenized codon in bold

